20th Australasian Fluid Mechanics Conference
Perth, Australia
5-8 December 2016

Boundedness of the velocity derivative flatness factor in a turbulent plane jet

S. L. Tang[1], R. A. Antonia[2], L. Djenidi[2], L. Danaila[3] and Y. Zhou[1]

[1]Institute for Turbulence-Noise-Vibration Interaction and Control, Shenzhen Graduate School
Harbin Institute of Technology, Shenzhen, 518055, P. R. China

[2]School of Engineering, University of Newcastle, NSW 2308, Australia

[3]CORIA CNRS UMR 6614, Université de Rouen, 76801 Saint Etienne du Rouvray, France

Abstract

This paper focuses on the statistics of normalized fourth-order moment of the longitudinal velocity derivative, $\partial u/\partial x$, i.e. the flatness factor $S_4 = \overline{(\partial u/\partial x)^4}/\overline{(\partial u/\partial x)^2}^2$ on the axis of a plane jet over a range of Taylor microscale Reynolds number varying between $R_\lambda \simeq 500$ and 1100. The aim is to determine the dependence of S_4 on R_λ. Different tests on the jet axis show that local isotropy is closely satisfied, allowing the use of $\bar{\varepsilon}_{iso}$, the locally isotropic form of the mean turbulent kinetic energy dissipation rate $\bar{\varepsilon}$.

The measurements show that S_4 remains approximately constant when $R_\lambda \geq 500$. This is inconsistent $S_4 \sim R_\lambda^\alpha$, where α is a small positive number, as predicted by various internal intermittency models. The constancy of S_4 is in full agreement with the relatively recent results (6) showing that S_3, the skewness of $\partial u/\partial x$, also tends to a constant when R_λ increases. The present results conform with the original similarity hypotheses of Kolmogorov (1).

Introduction

There is no doubt that the first two similarity hypotheses of Kolmogorov(1; 3), widely known as K41, and Kolmogorov's (1962) refined similarity hypothesis (2), or K62 - the latter was introduced to account for the so-called "internal intermittency" -, have had a huge impact on turbulence research. Various quantities, such as energy spectra and velocity structure functions, can be used to test either K41 or K62.

According to the K41 first hypothesis, these quantities adopt particular universal forms when the Taylor microscale Reynolds number, R_λ (=$u'\lambda/\nu$, where λ is the longitudinal Taylor microscale $u'/(\partial u/\partial x)'$ and a prime denotes a rms value) is very large. Interestingly, the Kolmogorov-normalized one-dimensional velocity spectra $\phi_u^*(k_1^*)$ (the asterisk denotes normalization by the Kolmogorov length scale, $\eta = (\nu^3/\bar{\varepsilon})^{1/4}$, where ν is the kinematic viscosity of the fluid; $\bar{\varepsilon}$ is the mean turbulent energy dissipation rate; the overline denotes time averaging, and/or Kolmogorov velocity scale, $u_K = (\nu\bar{\varepsilon})^{1/4}$) collapse in the high wavenumber region even when R_λ is as small as about 40 (4; 5).

In terms of the velocity structure functions, a major outcome of K41 is the prediction

$$\overline{(\delta u^*)^n} = f_{un}(r^*), \tag{1}$$

where the velocity increment $\delta u = u(x+r) - u(x)$ between two points separated by a distance r along x, (hereafter x is taken in the flow direction); f_{un} is a universal function when normalized by η and/or u_K for each value of n. When $r \to 0$, expression (1) yields the normalized moments of streamwise velocity derivatives, i.e.

$$S_n = \frac{\overline{(\partial u/\partial x)^n}}{\overline{(\partial u/\partial x)^2}^{n/2}}, \tag{2}$$

which, according to K41, should be constant for each value of n at large R_λ.

Following (7) and (8), many studies have focused on the evolution of S_n with R_λ with the view to testing K41 and K62. The majority of the work supports the argument that $|S_n|$ ($n \geq 3$) increases continuously with R_λ, viz.

$$|S_n| \sim R_\lambda^{\alpha(n)} \qquad (\alpha > 0), \tag{3}$$

e.g. (7; 8; 9; 10; 11). However, it appears now that not only the small-scale statistics are affected by R_λ (this is the so-call Finite Reynolds number effect, or FRN effect), when the latter is not large enough (12), but the approach towards an asymptotic state as R_λ increases differs from flow to flow (13; 6). These results indicate that the R_λ dependence on S_n should be revisited. And in particular, it should be assessed separately in each flow. Such attempts have been already initiated (6; 13; 14; 15). The latter authors derived the locally isotropic form of the transport equation for $\bar{\varepsilon}$, directly from the Navier-Stokes equations, in various turbulent flows, i.e. grid turbulence, along the axis in the self-preserving far-field of a round jet, along the centreline of a fully developed channel flow and a far-wake of a circular cylinder. They showed that, in each flow, the transport equation for $\bar{\varepsilon}$ can be expressed in the form

$$S_3 + 2\frac{G}{R_\lambda} = \frac{C}{R_\lambda}, \tag{4}$$

where G is the non-dimensional enstrophy destruction coefficient of $\bar{\varepsilon}$ defined by

$$G = \overline{u^2}\,\frac{\overline{(\partial^2 u/\partial x^2)^2}}{\overline{(\partial u/\partial x)^2}^2}. \tag{5}$$

In Eq. (4), analytical expressions for C differ from flow to flow. For example, in grid turbulence, C is equal to $\frac{90}{7(1+2R)}\left(\frac{n+1}{n}\right)$ with $R = \overline{v^2}/\overline{u^2}$ and n is the power-law decay exponent for the longitudinal velocity variance, viz. $\overline{u^2} \sim x^{-n}$ (6; 13) whereas, along the axis in the self-preserving far-field of a round jet, $C = \frac{90}{7(2+R)}$ (6; 13).

References (6; 14; 15) showed that since $2G/R_\lambda$ is found to be very nearly constant for $R_\lambda \geq 70 \sim 100$, S_3 approaches a universal constant, with a value of about 0.53, when R_λ is sufficiently large, but the way this constant is approached is flow dependent. In general, R_λ only needs to exceed about 300 for S_3 to become universal for all flows considered by Refs. (6; 14; 15). For Eq. (1), Pearson and Antonia (16) showed that $\overline{(\delta u^*)^2}$ collapses in

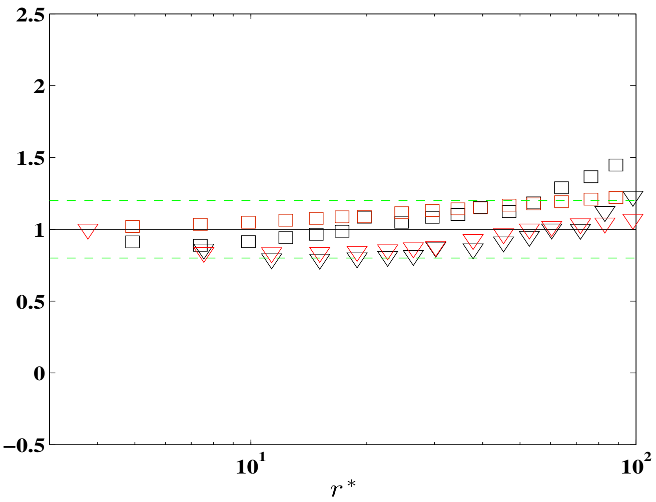

Figure 1: Ratios between the isotropic predictions and measured second- ($\overline{(\delta v)^2}_{iso}/\overline{(\delta v)^2}_{exp}$) and third- ($\overline{(\delta u)(\delta v)^2}_{iso}/\overline{(\delta u)(\delta v)^2}_{exp}$) order (black) structure functions in the dissipation range. $\bigtriangledown$, $R_\lambda = 1067$; ❏, $R_\lambda = 550$. Solid line indicates the isotropic ratio of 1. Dashed lines indicate a departure of 20% from the isotropic value of one.

the dissipative range over a large range of R_λ ($40 < R_\lambda < 4250$) and Antonia et al (6) showed that $S_{\delta u}$, the skewness of δu, viz. $S_{\delta u} = \overline{(\delta u)^3}/\overline{(\delta u)^2}^{3/2}$ also becomes universal in the dissipative range when R_λ is sufficiently large. The available evidence confirmed the constancy of Eq. (2) (K41) only for $n = 3$ and the universality of (1) (K41) in the dissipative range for $n = 2, 3$. The objective of this paper is to assess the R_λ dependence of Eqs. (1) and (2) for $n = 2-4$ in the dissipative range with the data in one flow (on the plane jet axis) over a relatively large range of R_λ (500 to 1100). The reason for choosing one flow, with a given initial condition, is that it allows the Reynolds number effect to be examined with minimal ambiguity. Naturally, further testing will be needed, in due course, in other flows and similar R_λ range.

Local isotropy

Before discussing the results, we first briefly assess local isotropy in this flow using the data of (17) and the following methods.

(1) Following (18), the well-known isotropic relation between second-order structure functions of longitudinal and transverse velocity components is given by

$$\overline{(\delta v)^2}_{iso} = \left(1 + \frac{r}{2}\frac{d}{dr}\right)\overline{(\delta u)^2}. \qquad (6)$$

The isotropic relation between third-order structure functions is given by (18)

$$\overline{(\delta u)(\delta v)^2}_{iso} = \left(\frac{1}{6}\frac{d}{dr} r\overline{(\delta u)^3}\right). \qquad (7)$$

Figure 1 shows the ratios between calculated and measured second- ($\overline{(\delta v)^2}_{iso}/\overline{(\delta v)^2}_{exp}$) and third- ($\overline{(\delta u)(\delta v)^2}_{iso}/\overline{(\delta u)(\delta v)^2}_{exp}$) order structure functions at R_λ=550 and 1067 respectively. For both the second- and third-order structure functions, the departure from local isotropy appears to be relatively small in the dissipation range ($r^* \leq 60$), the maximum departure being about 20%.

(2) A few statistics of $\omega_z (\equiv \partial v/\partial x - \partial u/\partial y)$ have been reported in (17). We simply note here that for local isotropy, the mean square value of $\overline{\omega_z^2}$, i.e. $\overline{(\partial v/\partial x)^2} + \overline{(\partial u/\partial y)^2} - 2\overline{(\partial v/\partial x)(\partial u/\partial y)}$ should be equal to $5\overline{(\partial u/\partial y)^2}$. The average measured value of $\overline{\omega_z^2}/\overline{(\partial u/\partial y)^2}$ is 4.5, also indicating a small (10%) departure from local isotropy. (3) In a far-wake of a circular cylinder, (19; 20) , who measured all components of $\bar{\varepsilon}$, observed a difference of about 30% between $\bar{\varepsilon}$ and $\bar{\varepsilon}_{iso}$ (=$15\nu\overline{(\partial u/\partial x)^2}$) and showed that only $\bar{\varepsilon}$ provided a satisfactory closure of the one-point energy budget. In this flow, (21; 15) applied the spectral chart method of (22) to estimate $\bar{\varepsilon}$ and found it to be very close to the true value of $\bar{\varepsilon}$. The spectral chart method of (22) has also been applied to the present plane jet spectra of u to obtain $\bar{\varepsilon}$. The results show that the estimates of $\bar{\varepsilon}$ are very close to $\bar{\varepsilon}_{iso}$, which allows us to use $\bar{\varepsilon}_{iso}$ for convenience.

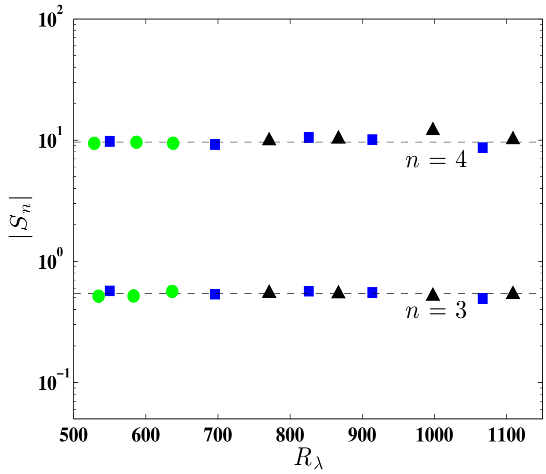

Figure 2: Dependence of S_n ($n = 3-4$) on R_λ on the axis of the plane jet. Green symbols, (23); black symbols, (16) (note that only the data for $f_c/f_K > 0.8$ are shown); blue symbols, (17) (each data point is an average of the two single hot-wire data points in the vorticity probe measurements). The horizontal dashed lines indicate the mean value of each of the plotted quantities.

Results

Figure 2 shows the variations of S_3 and S_4 with R_λ (Eq. (2)) on the axis of a plane jet. Detailed descriptions of the measurements in the plane jet are given in Refs. (23; 16; 17). Note that for the data of Pearson and Antonia (16), only those for which $f_c/f_K > 0.8$, where f_c is the low-pass filter cut-off frequency and f_K is the Kolmogorov frequency, are shown since an inadequate time resolution tends to underestimate S_3 (14). It can be seen from Fig. 2 that S_3 and S_4 are practically constant (by definition, $S_2 = 1$) over a range of R_λ ($500 < R_\lambda < 1100$) for these data sets, showing that the FRN effect is practically negligible for this range of R_λ. Antonia et al (24) showed that the magnitudes of S_3 and S_4 are 0.43 and 5.8 respectively on the axis of the plane jet at $R_\lambda = 160$; these are smaller than the values shown in Fig. 2 (0.54 and 9.8 respectively) suggesting that are likely to be influenced by the FRN effect.

We now focus on Eq. (1) up to $n = 4$ on the axis of a plane jet with the data of (17), bearing in mind that when $r \to 0$ we get S_n. Figure 3 shows $\overline{(\delta u^*)^n}$ ($n = 2-4$) for the plane jet data at

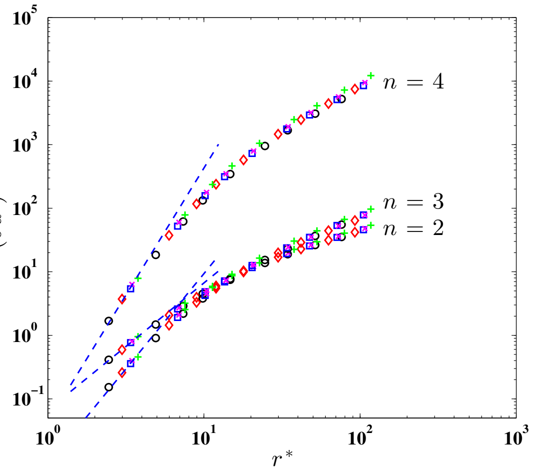

Figure 3: Kolmogorov-normalized structure function $\overline{(\delta u^*)^n}$ for $n=2-4$ along the axis of the plane jet at R_λ=550 (black), 696 (blue), 826 (red), 914 (pink), and 1067 (green) respectively(17). For clarity, only the data from one of the single hot-wires in vorticity probe are shown). The blue dashed lines correspond to $15^{-n/2}S_n r^n$ (S_n is the mean values shown in Fig. 2), i.e. approximate expression of Eq. (1) at small r^*.

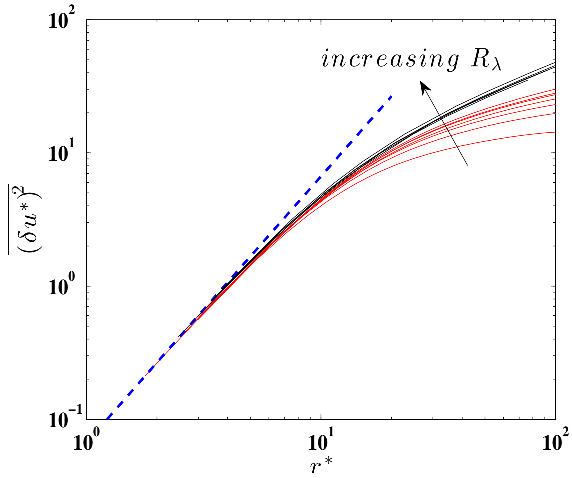

Figure 4: $\overline{(\delta u^*)^2}$ in plane jet (black curves). Also shown are the data (red curves) in grid turbulence (R_λ=27-100); detailed descriptions of the measurements are given in (25). The arrow points to the direction of increasing R_λ. The blue dashed line indicates $1/15r^{*2}$.

R_λ=550, 696, 826, 914, and 1067 respectively. We used $\bar{\varepsilon}_{iso}$ to estimate η and u_K since local isotropy is satisfied adequately in this flow. The blue dashed lines correspond to $15^{-n/2}S_n r^n$ (the values of S_n correspond to the averaged values shown in Fig. 2), i.e. the approximate form of Eq. (1) at small r^*. There is a relatively good collapse for all the structure functions at small r^*. Whilst the collapse for $n=2$, in good agreement with the observations of (16), may be criticised as being "somewhat contrived" since $\bar{\varepsilon}_{iso}$ is used to generate η and u_K, the previous discussion concerning the approximation $\bar{\varepsilon}_{iso} \approx \bar{\varepsilon}$ goes some way towards allaying this criticism. Further, the collapse for $n>2$, consistent with the trend in Fig. 2, is reasonably convincing at small r^*. For each value of n, the distributions collapse reasonably well at small r^* in compliance with Kolmogorov scaling. $\overline{(\delta u^*)^2}$ is replotted in a separate figure (Fig. 4) to provide a comparison with grid turbulence (R_λ=27-100), where local isotropy is satisfied adequately and $\bar{\varepsilon}$, as inferred from the energy budget, is in close agreement with $\bar{\varepsilon}_{iso}$ (a detailed description of the grid turbulence measurements is given in (25)). It can be seen from this figure that $\overline{(\delta u^*)^2}$ indeed collapses reasonably well for $r^*<10$ in both flows and follows the blue line at small r^*.

Theoretical considerations for the fourth-order moment

The constancy of S_3 at large R_λ in various flows has a solid analytical underpinning (6; 14; 15). Similarly, this section will focus primarily on the transport equations for the fourth-order moment in order to provide some analytical support for the independence of the Reynolds number for S_4 and $\overline{(\delta u^*)^4}$ in Figs. 2 and 3. According to (28; 29; 16), the pressure structure function in locally homogeneous and isotropic turbulence can be written solely in terms of fourth-order velocity structure functions as

$$\begin{aligned} D_p(r) = &-\tfrac{1}{3}D_{1111}(r)+\tfrac{4}{3}r^2\int_r^\infty y^{-3}[D_{1111}(y) \\ &+D_{\chi\chi\chi\chi}(y)-6D_{11\gamma\gamma}(y)]dy \\ &\tfrac{4}{3}\int_0^r y^{-1}[D_{\chi\chi\chi\chi}(y)-3D_{11\gamma\gamma}(y)]dy \end{aligned} \tag{8}$$

where $D_p(r)$ is the pressure structure function, $D_{1111}(r)$ (=$\overline{(\delta u)^4}$) is the fourth-order longitudinal velocity structure function, χ and γ stand for 2 or 3. The only assumption needed in deriving Eq. (8) is that turbulence is locally homogeneous and isotropic.

When $r\rightarrow 0$, Eq. (8) can be rewritten as follows (28; 29)

$$\begin{aligned} \frac{1}{\rho^2}\overline{\left(\frac{\partial p}{\partial x}\right)^2} = &\tfrac{4}{3}\int_0^\infty r^{-3}[D_{1111}(r) \\ &+D_{\chi\chi\chi\chi}(r)-6D_{11\gamma\gamma}(r)]dr. \end{aligned} \tag{9}$$

With Kolmogorov scaling, Eq. (9) can be further recast as

$$\begin{aligned} \overline{\left(\frac{\partial p^*}{\partial x^*}\right)^2} = &\tfrac{4}{3}\int_0^\infty r^{*-3}[D^*_{1111}(r^*) \\ &+D^*_{\chi\chi\chi\chi}(r^*)-6D^*_{11\gamma\gamma}(r^*)]dr^*. \end{aligned} \tag{10}$$

Because of the presence of r^{-3} in the integrands of (9) or (10), the dominant contributions from the integrals come from the dissipative range ($r^*<30$) (29). As shown in Fig. 3, the range of r^* over which $\overline{(\delta u^*)^4}$ collapses should increase as R_λ increases. The independence of $\overline{(\delta u^*)^4}$ in the dissipative range (Fig. 3) implies that the right side of (9) should approach a constant when R_λ is sufficiently large.

We now focus on the left side of Eq. (10). Several attempts have been made to estimate this term. For example, using the joint-Gaussianity approximation, Batchelor (30) obtained a value of about 1.3 for this term. A similar value (≈ 1.0) was obtained by Heisenberg (31). Pearson and Antonia (16) estimated this term in various flows over a large range of R_λ ($40<R_\lambda<1077$) and showed that it approaches a constant when $R_\lambda \approx 500$. Using the eddy-damped quasi-normal Markovian approximation, Meldi and Sagaut (33) also showed that the left side of Eq. (10) should approach a constant in freely decaying isotropic turbulence when R_λ is sufficiently large. It is not yet clear if the DNS values for this term will keep increasing with R_λ (e.g. (32)) or whether they will approach a constant as implied by the independence on R_λ of $\overline{(\delta u^*)^4}$ at small r^* (Fig. 3).

Conclusions

Relatively high Reynolds number data on the axis of a plane jet are analysed with the view to assess Reynolds number dependence of both the skewness (S_3) and the flatness (S_4) factors of the longitudinal velocity gradient. The data show strong evidence that both S_3 and S_4 are approximately constant when R_λ exceeds 500. Further, it is shown that Eq. (1) with $n = 2$, 3 and 4, is well verified in the dissipative range, which is consistent with the constancy of S_3 and S_4. Evidently, it would be desirable to carry out a similar analysis in regions away from the jet axis, and also examine the behaviour of S_3 and S_4 in other turbulent flows.

*

References

[1] A. N. Kolmogorov, Local structure of turbulence in an incompressible fluid for very large Reynolds numbers, *Dokl. Akad. Nauk SSSR*, **30**, 1941, 299–303.

[2] A. N. Kolmogorov, A refinement of previous hypotheses concerning the local structure of turbulence in a viscous incompressible fluid at high Reynolds number, *J. Fluid Mech.*, **13**, 1962, 82–85.

[3] A. N. Kolmogorov, Dissipation of energy in the locally isotropic turbulence, *Dokl. Akad. Nauk SSSR*, **32**, 19–21.

[4] S. G. Saddoughi and S . V . Veeravalli, Local isotropy of turbulent boundary layers at high Reynolds number, *J. Fluid Mech.*, **268**, 1994, 333–372.

[5] R. A. Antonia, L. Djenidi, and L. Danaila, Collapse of the turbulent dissipation range on Kolmogorov scales, *Phys. Fluids*, **26**, 2014, 045105.

[6] R. A. Antonia, S. L. Tang, L. Djenidi, and L. Danaila, Boundedness of the velocity derivative skewness in various turbulent flows, *J. Fluid Mech.*, **781**, 2015, 727–744.

[7] C. W. Van Atta and R. A. Antonia, Reynolds number dependence of skewness and flatness factors of turbulent velocity derivatives, *Phys. Fluids*, **23**, 1980, 52–257.

[8] K. Sreenivasan and R. A. Antonia, The phenomenology of small-scale turbulence, *Ann. Rev. Fluid Mech.*, **29**, 1997, 435–472.

[9] J. C. Wyngaard, *Turbulence in the atmosphere*, Cambridge University Press, 2010.

[10] J. C. Wyngaard and H. Tennekes, Measurements of the small-scale structure of turbulence at moderate Reynolds numbers, *J. Fluid Mech.*, **13**, 1970, 1962–1969.

[11] P. A. Davidson, *Turbulence: An introduction for scientists and engineers*, Oxford University Press, 2004.

[12] R. A. Antonia and P. Burattini, Approach to the 4/5 law in homogeneous isotropic turbulence, *J. Fluid Mech.*, **550**, 2006, 175–184.

[13] F. Thiesset, R. A. Antonia and L. Djenidi, Consequences of self-preservation on the axis of a turbulent round jet, *J. Fluid Mech.*, **748**, 2014, R2.

[14] S. L. Tang, R. A. Antonia, L. Djenidi, H. Abe, T. Zhou, L. Danaila, and Y. Zhou, Transport equation for the mean turbulent energy dissipation rate on the centreline of a fully developed channel flow, *J. Fluid Mech.*, **777**, 2015, 151–177.

[15] S. L. Tang, R. A. Antonia, L. Djenidi, and Y. Zhou, Transport equation for the isotropic turbulent energy dissipation rate in the far-wake of a circular cylinder, *J. Fluid Mech.*, **784**, 2015, 109–129.

[16] B. R. Pearson and R. A. Antonia, Reynolds-number dependence of turbulent velocity and pressure increments, *J. Fluid Mech.*, **444**, 2001, 343–382.

[17] T. Zhou, R. A. Antonia, and L. P. Chua, Flow and Reynolds number dependencies of one-dimensional vorticity fluctuations, *Journal of Turbulence*, **28**, 2005.

[18] A. S. Monin and A. M. Yaglom, *Statistical fluid dynamics*, Vol. 2. MIT., 2007.

[19] R. A. Antonia and L. W. Browne, Anisotropy of temperature dissipation in a turbulent wake, *J. Fluid Mech.*, **163**, 1986, 393–403.

[20] L. W. Browne, R. A. Antonia, and D. A. Shah, Turbulent energy dissipation in a wake, *J. Fluid Mech.*, **179**, 1987, 307–326.

[21] S. L. Tang, R. A. Antonia, L. Djenidi, and Y. Zhou, Complete self-preservation along the axis of a circular cylinder the far-wake, *J. Fluid Mech.*, **786**, 2015, 253–274.

[22] L. Djenidi and R. A. Antonia, A spectral chart method for estimating the mean turbulent kinetic energy dissipation rate, *Exp. Fluids*, **53**, 2012, 1005–1013.

[23] R. A. Antonia, A. J. Chambers, and B. R. Satyaprakash, Reynolds number dependence of high-order moments of the streamwise turbulent velocity derivative, *Boundary-Layer Meteorol*, **21**, 1981, 159?171.

[24] R. A. Antonia, F. Anselmet, and A. J. Chambers, Assessment of local isotropy using measurements in a turbulent plane jet, *J. Fluid Mech.*, **163**, 1986, 365–391.

[25] T. Zhou and R. A. Antonia, Reynolds number dependence of the small-scale structure of grid turbulence, *J. Fluid Mech.*, **406**, 2000, 81–107.

[26] P. Tabeling, G. Zocchi, F. Belin, J. Maurer, and H. Willaime, Probability density functions, skewness, and flatness in large Reynolds number turbulence,*Phys. Rev. E*, **53**, 1996, 1613–1621.

[27] F. Belin, J. Maurer, P. Tabeling, and H. Willaime, Velocity gradient distributions in fully developed turbulence: experimental study, *Phys. Fluids*, **9**, 1997, 3843–3850.

[28] R. J. Hill and J. M. Wilczak, Pressure structure functions and spectra for locally isotropic turbulence, *J. Fluid Mech.*, **296**, 1995, 247–269.

[29] P. Vedula and P. K. Yeung, Similarity scaling of acceleration and pressure statistics in numerical simulations of isotropic turbulence, *Phys. Fluids*, **11**, 1999, 1208–1220.

[30] G. K. Batchelor, Pressure fluctuations in isotropic turbulence, *Proc. Camb. Phil. Soc.* , **47**, 1951, 359–374.

[31] W. Heisenberg, Zur Statischen Theorie der Turbulenz, *Z. Phys.*, **124**, 1948, 628–657.

[32] D. A. Donzis, K. R. Sreenivasan and P. K. Yeung, Some results on the Reynolds number scaling of pressure statistics in isotropic turbulence, *Physica D*, **241**, 2012, 164–168.

[33] M. Meldi and P. Sagaut, Pressure statistics in self-similar freely decaying isotropic turbulence, *J. Fluid Mech.*, **717**, 2013, R2.